Numer. Math. Theor. Meth. Appl.
doi: 10.4208/nmtma.2015.w09si

Vol. **8**, No. 2, pp. 237-252
May 2015

A Multigrid Solver based on Distributive Smoother and Residual Overweighting for Oseen Problems

Long Chen[1,*], Xiaozhe Hu [4], Ming Wang [3], and Jinchao Xu [2]

[1] *Department of Mathematics, University of California at Irvine. Irvine, CA, 92697, USA.*
[2] *Department of Mathematics, Pennsylvania State University, University Park, PA 16801, USA.*
[3] *LMAM, School of Mathematical Sciences, Peking University, Beijing 100871, China.*
[4] *Department of Mathematics, Tufts University, Medford, MA 02155.*

Received 22 November 2013; Accepted 25 September 2014

Abstract. An efficient multigrid solver for the Oseen problems discretized by Marker and Cell (MAC) scheme on staggered grid is developed in this paper. Least squares commutator distributive Gauss-Seidel (LSC-DGS) relaxation is generalized and developed for Oseen problems. Residual overweighting technique is applied to further improve the performance of the solver and a defect correction method is suggested to improve the accuracy of the discretization. Some numerical results are presented to demonstrate the efficiency and robustness of the proposed solver.

Key words: Navier-Stokes equations, LSC-DGS, multigrid.

1. Introduction

We consider multigrid (MG) methods for the following linearized steady-state incompressible Navier-Stokes (NS) equations (Oseen model) in two dimensions:

$$\begin{cases} -\mu\Delta \boldsymbol{u} + (\boldsymbol{a}\cdot\nabla)\boldsymbol{u} + \nabla p = \boldsymbol{f}, & \text{in } \Omega, \\ \nabla\cdot\boldsymbol{u} = 0, & \text{in } \Omega, \\ \boldsymbol{u} = \boldsymbol{g}, & \text{on } \partial\Omega, \end{cases} \tag{1.1}$$

where $\mu = 1/Re$, with Re the Reynold number, $\boldsymbol{u} = (u,v)^t$ is the velocity, $\boldsymbol{a} = (a(x,y), b(x,y))^t$ is the flow function satisfying $\operatorname{div}\boldsymbol{a} = 0$, $\boldsymbol{g}$ is the boundary data, and $\boldsymbol{f} = (f_1, f_2)^t$ is the external force. This linearized model usually comes from using the Picard's iteration to solve the NS equation, see, e.g. [13] (Section 7.2.2).

*Corresponding author. *Email addresses:* chenlong@math.uci.edu (Long Chen), xiaozhe.hu@tufts.edu (Xiaozhe Hu), wangming.pku@gmail.com (Ming Wang), xu@math.psu.edu (Jinchao Xu).

 ©2015 Global-Science Press

https://doi.org/10.4208/nmtma.2015.w09si Published online by Cambridge University Press

Spatial discretization of the Oseen model (1.1) using either finite element or finite difference method leads to a large-scale sparse saddle point system of the following matrix form

$$\begin{pmatrix} F & B' \\ B & 0 \end{pmatrix} \begin{pmatrix} \boldsymbol{u} \\ p \end{pmatrix} = \begin{pmatrix} \boldsymbol{f} \\ 0 \end{pmatrix}, \tag{1.2}$$

where $\boldsymbol{u}$ now denotes the discrete velocity, p denotes the discrete pressure, F is the discretization of $-\mu\Delta + (\boldsymbol{a} \cdot \nabla)$, B' is the discrete gradient, and B is the (negative) discrete divergence.

Much work has been done for developing efficient solvers for (1.2), especially efficient preconditioners for Krylov subspace methods based on the block matrix form, see, e.g. [1, 13] and references therein. Multigrid methods have also been considered, for example [6, 14, 16, 18, 19, 22, 24, 25, 33]. We are interested in efficient MG methods that are robust with respect to both the mesh size h and the Reynold number Re.

For low Reynold number flow, John et. [18, 19] use multiple discretizations which combines a higher order finite element discretization with a lower order finite element approximation as a coarse grid solver. In [14], Fuchs and Zhao considered the distributive Gauss-Seidel (DGS) smoother and have shown that MG method using the DGS smoother works for enclosed flows in three dimensions with low Re numbers.

For high Reynolds number, the Oseen model becomes convection dominated and development of robust MG methods becomes more and more challenging. Brandt and Yavneh [6] propose a MG solver combined with a DGS smoother for high-Reynolds incompressible entering flows. They use standard or narrow upwind schemes of first or second order to discretize the convection term. Similar to the DGS smoother for Stokes problem [5], a good pressure convection-diffusion operator which almost commutes with the divergence operator is constructed to design an efficient DGS smoother. Based on such smoother, Thomas, Diskin and Brandt [24] obtain textbook multigrid efficiency for a model problem of flow past a finite flat plate. However, in this work, the construction of the pressure convection-diffusion operator is done for special flows, essentially constant flows, and it is not easy to generalize such construction to general flows. In [33], Zhang develop a MG solver with a second order upwind scheme for the convection term. Vanka smoother [25] with under-relaxation is used which is not robust with respect to the Re number. The number of iterations of MG cycles increases dramatically when Re number increases, i.e. $5 \sim 300$ steps with Re number from the range of $100 \sim 5000$. In [16], Hamilton, Benzi, and Haber considered MG methods for the Marker-and-Cell (MAC) discretization using smoothers based on Hermition/skew-Hermitian (HSS) and augmented Lagrangian (AL) splittings. For steady state Oseen problem, the proposed MG methods show moderate degeneracy on the Reynolds number up to $Re = 2048$.

In this paper, we consider least-square commutator distributive Gauss-Seidel (LSC-DGS) relaxation for solving the Oseen equation discretized by the MAC discretization with a first order upwind scheme. Central difference stencils are used for both convection and diffusion operators. To stabilize the scheme, the viscosity μ is replaced

https://doi.org/10.4208/nmtma.2015.w09si Published online by Cambridge University Press

by a numerical viscosity $\mu_h = h\|\boldsymbol{a}\|_\infty/2$. LSC-DGS smoother, first proposed in [26] for Stokes problems, constructs the commutator in a purely algebraic way and, therefore, automatically provides a convection-diffusion operator for the pressure variable that can be used in the DGS smoothers. The first order upwind scheme depends on the mesh size h and thus the coarse grid problem is not the original problem considered in the fine mesh. To minimize the discrepancy between levels, we apply $\mathcal{W}$-cycle method based the overweighting technique proposed in [7]. According to the numerical results, the resulting $\mathcal{W}$-cycle MG methods is robust and efficient for the first order upwind MAC discretization.

Ideally fast solvers should be incorporated with the discretization to achieve certain accuracy with nearly optimal computational complexity [3]. Our solver developed in this work, however, is limited to the first order upwinding scheme. We expect the MG solver based on the LSC-DGS smoother for the first order upwinding scheme can be used as a preconditioner or in the defect-correction procedure for other high order stable or unstable discretizations on the same rectangular grids or other unstructured grids. In this paper, we explore the potential along this direction by considering a simple example. We apply defect-correction [4, 15] framework to a central difference discretization, which is known to be a second order but unstable scheme, on the same rectangular grid. In one defect correction iteration, only few $\mathcal{W}$-cycles for the first order upwind discretization are applied. The numerical results for a second order unstable discretization show that the defect-correct procedure improves the overall accuracy within several MG iterations.

The rest of the paper is organized as follows. In section 2, we construct LSC-DGS smoother for the Oseen problem. In section 3, we present the $\mathcal{W}$-cycle with residual overweighting and in section 4, we present the defect-correction method. In section 5, we provide several numerical examples to show the robustness and efficiency of our MG solver.

2. LSC-DGS Smoother for the Oseen Problem

In this section, we generalize the LSC-DGS smoother [26] designed for the Stokes equations to the Oseen problem.

2.1. Discretization

The system (1.1) can be written in the operator form:

$$\begin{pmatrix} -\mu\Delta + \boldsymbol{a}\cdot\operatorname{grad} & \operatorname{grad} \\ -\operatorname{div} & 0 \end{pmatrix} \begin{pmatrix} \boldsymbol{u} \\ p \end{pmatrix} = \begin{pmatrix} \boldsymbol{f} \\ 0 \end{pmatrix} \tag{2.1}$$

We discretize system (2.1) with (Marker and Cell) MAC scheme on a staggered grid (see Fig. 1) and obtain the following matrix form

$$\begin{pmatrix} F & B' \\ B & 0 \end{pmatrix} \begin{pmatrix} \boldsymbol{u} \\ p \end{pmatrix} = \begin{pmatrix} \boldsymbol{f} \\ 0 \end{pmatrix}, \quad \text{or simply} \quad \mathcal{L}\boldsymbol{x} = \boldsymbol{b}. \tag{2.2}$$

https://doi.org/10.4208/nmtma.2015.w09si Published online by Cambridge University Press

In order to avoid introducing more notation, we also use $\boldsymbol{u}, p$ and $\boldsymbol{f}$ as vectors when there is no ambiguity. F and B are the central differential approximations of operators $-\mu_h\Delta + \boldsymbol{a}\cdot\operatorname{grad}$ and $-\operatorname{div}$ respectively with the numerical viscosity $\mu_h = h\|\boldsymbol{a}\|_\infty/2$.

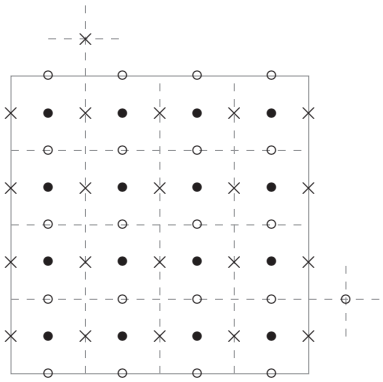


Figure 1: Location of unknowns on a staggered grid. The discrete pressure p is defined at cell centers ($\bullet$). The discrete velocity u and v are defined at vertical edges centers ($\times$) and horizontal edges centers ($\circ$), respectively.

It is well known that for convection dominated convection-diffusion operators $-\mu\Delta + \boldsymbol{a}\cdot\operatorname{grad}$, the central difference scheme leads to a unstable scheme. To stabilize the discretization, we change the viscosity μ to a numerical viscosity $\mu_h = h\|\boldsymbol{a}\|_\infty/2$ which results in a first order upwind scheme. The stencil for the horizontal velocity u is

$$\frac{h\|\boldsymbol{a}\|_\infty}{2}\begin{bmatrix} & -1 & \\ -1 & 4 & -1 \\ & -1 & \end{bmatrix} + \frac{ha}{2}\begin{bmatrix} & 0 & \\ -1 & 0 & 1 \\ & 0 & \end{bmatrix},$$

and the stencil for the vertical velocity v is

$$\frac{h\|\boldsymbol{a}\|_\infty}{2}\begin{bmatrix} & -1 & \\ -1 & 4 & -1 \\ & -1 & \end{bmatrix} + \frac{hb}{2}\begin{bmatrix} & 1 & \\ 0 & 0 & 0 \\ & -1 & \end{bmatrix}.$$

This guarantees that the matrix F is an M-matrix and Gauss-Seidel iteration without special ordering converges for computing F^{-1}. We do not use the standard upwinding stencil for the convection term, i.e., one sided difference based on the sign of $\boldsymbol{a}$, which also leads to an M-matrix discretization of operator F. This is due to the fact that the commutator in the smoother to be developed in Section 2.3 will be small only if central difference stencils are used for both convection and diffusion operators.

2.2. Distributive Gauss-Seidel Smoother

An iterative method for solving the linear system (2.2) can be written in the following general formulation, starting from an initial guess $\boldsymbol{x}^0$, for $k = 0, 1, 2, \ldots,$

$$\boldsymbol{x}^{k+1} = \boldsymbol{x}^k + \mathcal{R}(\boldsymbol{b} - \mathcal{L}\boldsymbol{x}^k), \tag{2.3}$$

https://doi.org/10.4208/nmtma.2015.w09si Published online by Cambridge University Press

where $\mathcal{R}$ is an approximation of $\mathcal{L}^{-1}$. Note that, we may need to include a scaling factor into $\mathcal{R}$ in order to ensure the iterative method is convergent, i.e., $\rho(\mathcal{I}-\mathcal{R}\mathcal{L})<1$ where $\mathcal{I}$ denotes identity matrix and $\rho(\cdot)$ denotes the spectral radius. Using $\mathcal{R}$ as an iterative method may be very slow, i.e., $\rho(\mathcal{I}-\mathcal{R}\mathcal{L})$ could be very close to one, say $1-Ch^2$. However to be an effective smoother, $\mathcal{R}$ only needs to reduce the high frequency part of the error.

Effective smoothers for Stokes and Navier-Stokes equations include distributive Gauss-Seidel (DGS) smoothers [5], incomplete LU decomposition for a transformed system [27, 28], block Jacobi and Gausss-Seidel smoother which is better known as Vanka smoother [25], constrained smoother by Braess and Sarazin [2], and smoothers based on the Hermitian/skew-Hermitian (HSS) and augmented Lagrangian (AL) splittings [16] etc. We refer to the review [22] for a more completed list.

We shall construct an effective DGS type smoother for the Oseen problem. The standard relaxations, e.g., the Gauss-Seidel relaxation, are not applicable to the system (2.2). This is because the 2×2 matrix $\mathcal{L}$ is not diagonally dominant and especially one diagonal block is zero. The idea of the distributive relaxation is to transform the principle operators to the main diagonal and apply the equation-wise decoupled relaxation. We first recall the traditional DGS smoother applied to the Oseen problem. In [5], Brandt and Dinar introduced a distributive matrix

$$\mathcal{M}=\begin{pmatrix} I & B' \\ 0 & -F_p \end{pmatrix},$$

where F_p is a suitable approximation of the convection-diffusion operator $-\mu\Delta+a\partial_x+b\partial_y$ for the pressure. Multiplying $\mathcal{M}$ to the right of $\mathcal{L}$, we have

$$\mathcal{L}\mathcal{M}=\begin{pmatrix} F & FB'-B'F_p \\ B & BB' \end{pmatrix}\approx\begin{pmatrix} F & 0 \\ B & BB' \end{pmatrix}=:\widetilde{\mathcal{L}\mathcal{M}}$$

and consequently

$$\mathcal{L}^{-1}=\mathcal{M}(\mathcal{L}\mathcal{M})^{-1}\approx\mathcal{M}\widetilde{\mathcal{L}\mathcal{M}}^{-1}.$$

Now the approximation of the transformed operator $\widetilde{\mathcal{L}\mathcal{M}}$ is diagonally dominant (indeed lower triangular) and thus can be easily solved or relaxed. Suppose $\widetilde{\mathcal{L}\mathcal{M}}$ is further approximated by

$$\mathcal{S}=\begin{pmatrix} S_u & 0 \\ B & S_p \end{pmatrix}, \tag{2.4}$$

where S_u and S_p are effective smoothers for F and $A_p:=BB'$, respectively. Note that for the MAC scheme, A_p is the discrete (negative) Laplacian operator $-\Delta_p$ for pressure with Neumann boundary condition. The matrix $\mathcal{M}\mathcal{S}^{-1}$ will introduce an effective smoother for the original system (2.2):

$$\boldsymbol{x}^{k+1}=\boldsymbol{x}^k+\mathcal{M}\mathcal{S}^{-1}(\boldsymbol{b}-\mathcal{L}\boldsymbol{x}^k). \tag{2.5}$$

https://doi.org/10.4208/nmtma.2015.w09si Published online by Cambridge University Press

The name distributive relaxation comes from the fact that the correction $\mathcal{S}^{-1}(\boldsymbol{b}-\mathcal{L}\boldsymbol{x}^k)$ in (2.5) is distributed over the entries of $\boldsymbol{x}^{k+1}$ through the distributive matrix $\mathcal{M}$.

In the construction of a distributive smoother, we neglect the $(1,2)$ block of the transformed system. This can be justified if the commutator $FB'-B'F_p$ is small in magnitude or is of low rank. Therefore, how to construct such operator F_p is the key to the success of the traditional DGS relaxation. For entering flows, in [6], Brandt and Yavneh proposed a construction of such F_p and numerically verify its efficiency. For general flows, such as enclosed or recirculating flow, the construction of operator F_p is less straightforward.

2.3. Least-Square Commutators Distributive Gauss-Seidel Relaxation

As mentioned before, the crucial part of the DGS relaxation is how to choose F_p such that the commutator $FB'-B'F_p$ is as small as possible. One natural approach is to minimize the commutator $FB'-B'F_p$ in certain norm which leads to the LSC-DGS smoother proposed in [26] for Stokes equations. We adopt this idea here and develop a LSC-DGS smoother for the Oseen problem.

To this end, we solve the following minimization problem

$$\min_X E(X)=\min_X \|FB'-B'X\|_{\mathcal{F}}, \tag{2.6}$$

where $\|\cdot\|_{\mathcal{F}}$ denotes the Frobenius norm (F-norm) of matrices. By simple calculation [13], we have

$$F_p:=\arg\min_X E(X)=(BB')^{-1}BFB'.$$

With such choice of F_p, we have

$$\mathcal{M}=\begin{pmatrix} I & B' \\ 0 & -(BB')^{-1}BFB' \end{pmatrix},$$

and

$$\mathcal{L}\mathcal{M}=\begin{pmatrix} F & FB'-B'F_p \\ B & BB' \end{pmatrix}=\begin{pmatrix} F & PFB' \\ B & BB' \end{pmatrix}$$

where $P=I-B'(BB')^{-1}B$ is the l_2-projection to the div-free space. Since the $ker(B)$ is orthogonal to the range of B', we have $PB'=0$ and consequently, $PFB'=P(FB'-B'X)$ for any $X:\mathbb{R}^{N_p}\to\mathbb{R}^{N_p}$, where N_p is the dimension of the pressure space. This means that, with this special choice of F_p, we do our best to minimize the effect of the $(1,2)$ block of the transformed matrix.

Whether the PFB' is negligible or not will depend on the discretization. This is the main motivation we chose MAC as our discretization. It can be verified by direct calculation that

$$\Delta B'=B'\Delta_p \tag{2.7}$$

for standard central difference stencils. Due to the Dirichlet boundary condition, the stencil for the near boundary nodes of velocity will be modified and thus violates the

https://doi.org/10.4208/nmtma.2015.w09si Published online by Cambridge University Press

commutative relation. But for interior nodes or periodic boundary condition, (2.7) holds. Therefore the commutator is small for the diffusion part. For the convection part, it is also straight forward to verify that for a constant flow $(\boldsymbol{a}\cdot\nabla)B' = B'(\nabla\cdot\boldsymbol{a})$ when the central difference stencil is used. Therefore we could expect the commutator for the convection term is small when $\boldsymbol{a}$ is smooth.

We then have

$$\mathcal{L}\mathcal{M} \approx \begin{pmatrix} F & 0 \\ B & BB' \end{pmatrix} =: \widetilde{\mathcal{L}\mathcal{M}}.$$

Similar to the traditional DGS relaxation, we use

$$\mathcal{M}\widetilde{\mathcal{L}\mathcal{M}}^{-1} = \begin{pmatrix} I & B' \\ 0 & -(BB')^{-1}BFB' \end{pmatrix} \begin{pmatrix} F & 0 \\ B & BB' \end{pmatrix}^{-1}$$

as an approximation of $\mathcal{L}^{-1}$. The matrix $\mathcal{M}\mathcal{S}^{-1}$ will introduce an effective smoother for the original system (2.2) where $\mathcal{S}$ is given in (2.4). The $(BB')^{-1}$ in the $(2,2)$ block of $\mathcal{M}$ will be replaced by an effective smoother also. Since the least square commutator is used to design the distributive matrix, we call the resulting smoother Least-Squares Commutator DGS (LSC-DGS) smoother. One iteration of LSC-DGS smoother can be performed by the following algorithm.

Algorithm 1. LSC-DGS Smoother $[\boldsymbol{u}^{k+1}, p^{k+1}] \leftarrow \texttt{LSC-DGS}(\boldsymbol{u}^k, p^k)$

1. Relax the momentum equation

$$\boldsymbol{u}^{k+\frac{1}{2}} = \boldsymbol{u}^k + S_u^{-1}(\boldsymbol{f} - A\boldsymbol{u}^k - B'p^k),$$

2. Relax the transformed continuity equation

$$\delta q = S_p^{-1}(0 - B\boldsymbol{u}^{k+\frac{1}{2}}).$$

3. Distribute the correction back to the original variables

$$\begin{aligned} \boldsymbol{u}^{k+1} &= \boldsymbol{u}^{k+\frac{1}{2}} + B'\delta q, \\ p^{k+1} &= p^k - S_p^{-1}BFB'\delta q. \end{aligned}$$

Since A_p is a discrete Laplacian operator for the pressure, smoother S_p can be chosen as a (symmetric) Gauss-Seidel iteration and can be implemented in an algebraic way by forming A_p explicitly. When applicable, red-black or general multi-coloring ordering can be further applied to improve the smoothing effect. Thanks to the first order upwind scheme we use, the matrix F is an M-matrix and thus S_u can be also chosen as a symmetric Gauss-Seidel iteration. No special ordering is needed.

https://doi.org/10.4208/nmtma.2015.w09si Published online by Cambridge University Press

Compared with the standard DGS (i.e. an explicit F_p or its action is constructed a priori), step 3 of LSC-DGS requires one more relaxation and one more matrix-vector multiplication. On the other hand, LSC-DGS can be implemented using existing matrices without further intelligent investigation.

We want to point out that the LSC-DGS smoother is closely related to the block preconditioner proposed in [11, 12]. The LSC was firstly developed by Elman [11], and used to construct a least-squares approximation to the Schur complement of the linearized Navier-Stokes system, yielding the so-called BFBt preconditioner. Elman, Howle, Shadid, Shuttleworth, and Tuminaro [12] improved the LSC by using scaling of mass matrices, together with methods of computing sparse approximate inverses. For the MAC scheme, the mass matrix is a scaling of the identity matrix and thus not needed in our construction.

3. $\mathcal{W}$-cycle Multigrid with Overweighting

Recall that, in order to obtain a stable discretization for high Reynolds number, i.e. small viscosity μ, we consider a first order upwind scheme by replacing μ by $\mu_h = h\|\boldsymbol{a}\|_\infty/2$. Namely, we solve the following Oseen problem

$$\mathcal{L}^h \boldsymbol{x}^h = \begin{pmatrix} -\mu_h\Delta + \boldsymbol{a}\cdot\operatorname{grad} & \operatorname{grad} \\ -\operatorname{div} & 0 \end{pmatrix} \begin{pmatrix} \boldsymbol{u}^h \\ p^h \end{pmatrix} = \boldsymbol{b}^h \tag{3.1}$$

discretized by the standard MAC scheme. Note that, the operator $\mathcal{L}^h$ depends on the mesh size h on each level. Careful consideration is needed for designing efficient MG method for solving such linear systems. The continuation of the numerical viscosity will be explored in a multilevel fashion.

In [7], Brandt and Yavneh developed a $\mathcal{W}$-cycle with overweighting for the convection-dominated convection-diffusion equation discretized by a stable first order discretization. The idea is to overweight the coarse grid correction based on the local mode analysis. Here, we adopt such idea to the Oseen equation.

Denote $\mathcal{T}_h$ as the grid with mesh size h and $\mathcal{T}_H$ as the coarse grid with $H = 2h$. Denote the standard prolongation and restriction operator as $\mathcal{I}_H^h$ and $\mathcal{I}_h^H$. In stencil notation, the restriction operators are ($*$ indicates the position of the coarse-grid point)

$$(I_h^H)_u = \frac{1}{8}\begin{pmatrix} 1 & 2 & 1 \\ & * & \\ 1 & 2 & 1 \end{pmatrix}, \quad (\mathcal{I}_h^H)_v = \frac{1}{8}\begin{pmatrix} 1 & & 1 \\ 2 & * & 2 \\ 1 & & 1 \end{pmatrix}, \quad (\mathcal{I}_h^H)_p = \frac{1}{4}\begin{pmatrix} 1 & & 1 \\ & * & \\ 1 & & 1 \end{pmatrix}.$$

The prolongation will be the transpose of the restriction. Note that on the coarse grid $\mathcal{T}_H$, we are inverting the operator $\mathcal{L}^H$ which is different from $\mathcal{L}_h^H$, the discretization of $\mathcal{L}^h$ restricted to the coarse grid. A weight greater than one (overweighting) is applied to the coarse grid correction to minimize the discrepancy of this inconsistency.

The $\mathcal{W}$-cycle with overweighting is defined in Algorithm 2 as follows.

https://doi.org/10.4208/nmtma.2015.w09si Published online by Cambridge University Press

Algorithm 2. $\mathcal{W}$-cycle with overweighting: $\boldsymbol{x}^h \leftarrow \texttt{W_ow}(\mathcal{L}^h, \boldsymbol{b}^h, \boldsymbol{x}^h)$

1. Relax s_1 steps on $\mathcal{L}^h \boldsymbol{y}^h = \boldsymbol{b}^h$ with initial guess $\boldsymbol{x}^h$.
2. Transfer residual to the coarse grid H

$$\boldsymbol{r}_1^H = \mathcal{I}_h^H(\boldsymbol{b}^h - \mathcal{L}^h \boldsymbol{x}^h),$$

and solve the coarse grid problem $\mathcal{L}^H \boldsymbol{e}_1^H = \boldsymbol{r}_1^H$, approximately by one step of $\mathcal{W}$-cycle on the coarse grid, i,e,

$$\boldsymbol{e}_1^H \leftarrow \texttt{W_ow}(\mathcal{L}^H, \boldsymbol{r}_1^H, \boldsymbol{0}).$$

3. Modify the right hand side of the coarse grid problem,

$$\boldsymbol{r}_2^H = \boldsymbol{r}_1^H + (\mathcal{L}^H - \boldsymbol{\alpha}\mathcal{L}_h^H)\boldsymbol{e}_1^H,$$

then solve the following coarse grid problem $\mathcal{L}^H \boldsymbol{e}_2^H = \boldsymbol{r}_2^H$, approximately by another step of $\mathcal{W}$-cycle, i.e.,

$$\boldsymbol{e}_2^H \leftarrow \texttt{W_ow}(\mathcal{L}^H, \boldsymbol{r}_2^H, \boldsymbol{0}).$$

Here $\boldsymbol{\alpha} = \text{diag}(\alpha_u I, \alpha_p I)$.

4. Interpolate and add $\boldsymbol{e}_2^H$ to $\boldsymbol{x}^h$, comply with s_2 post-smoothing steps.

$$\boldsymbol{x}^h = \boldsymbol{x}^h + \boldsymbol{\alpha}\mathcal{I}_H^h \boldsymbol{e}_2^H.$$

Following the methodology proposed in [7], the scaling factor α_u and α_p can be computed by the local mode analysis and optimization for minimizing the error amplification factors. As the procedure is similar to [7], we skip the details here and refer interested readers to [7] for the detailed derivation. In the numerical results we showed below, we choose $\alpha_u = 4/3$ and $\alpha_p = 1$. Such choice makes sense because the convection-diffusion operator mainly applies on $\boldsymbol{u}$, therefore, only the velocity needs certain overweighting to minimize the discrepancy between the levels due to the stabilized diffusion coefficients. For the pressure, the overweighting is unnecessary.

Residual overweighting technique tries to achieve a compromise between fully and partially corrected error components in the coarse grid correction step by overweighting the residuals. As pointed out in [7, 30], residual overweighting technique works well for scalar convection problems and can be applied to convection-like problems individually with careful choice of the weights depend on alignment between grid lines and flow characteristics. In [31], overweighting technique is combined with upstream discretization and downstream relaxation and efficient MG method (even V-cycle) has

https://doi.org/10.4208/nmtma.2015.w09si Published online by Cambridge University Press

been developed for advection problems with closed characteristics. However, the overweighting is optimal without physical diffusions and may have problems for convection-diffusion problems with significant physical diffusions. Therefore, special attention is needed when applying the overweighting technique to NS equations, especially with wide variation of the Reynolds number.

There are other approaches to improve the coarse-grid approximation. For example, [10] proposed a modified coarse-grid operator for scalar convection problems, and [23] apply Krylov-subspace acceleration methods with MG methods for convection-diffusion and Navier-Stokes problems. In general, conditions on effective coarse-grid discretization can be found in [30]. On the other hand, "global" relaxations, such as ILU and line smoothers, are also used to reduce the smooth error components that can not be well corrected on coarse grid, see [21, 32].

4. Defect Correction Procedure

The $\mathcal{W}$-cycle MG method developed in the previous section is for the first order upwind MAC scheme. In practice, the accuracy of such first order scheme usually is not satisfactory and the biggest Reynolds such first order scheme can handle is limited by the mesh size h. In order to improve the accuracy, we apply the defect correction technique, see, e.g. [4, 15].

The idea is that we consider a high order discretization, which shares the same degree of freedoms (DoFs) with the MAC scheme, for the original Oseen model (1.1) on the same grid. We denote it by

$$\bar{\mathcal{L}}^h \bar{\boldsymbol{x}}^h = \bar{\boldsymbol{b}}^h.$$

Note that, the high order discretization $\bar{\mathcal{L}}^h$ can be either stable or unstable and it is used to improve the accuracy of the first order upwind MAC scheme $\mathcal{L}^h$ by the following defect correction procedure.

$$\begin{aligned}
&\boldsymbol{x}_0^h = \left(\mathcal{L}^h\right)^{-1} \boldsymbol{b}^h;\\
&\boldsymbol{x}_k^h = \boldsymbol{x}_{k-1}^h + \left(\mathcal{L}^h\right)^{-1} \left(\bar{\boldsymbol{b}}^h - \bar{\mathcal{L}}^h \boldsymbol{x}_{k-1}^h\right),\ k = 1, 2, \cdots.
\end{aligned}$$

It is easy to see that if

$$\rho\left(\mathcal{I} - \left(\mathcal{L}^h\right)^{-1} \bar{\mathcal{L}}^h\right) < 1,$$

the above defect correction iteration will converge to $\bar{\boldsymbol{x}}^h$ as $k \mapsto \infty$ which might be a unstable solution of the Oseen problem because we do not require the high order discretization $\bar{\mathcal{L}}^h$ be stable. Therefore, as suggested in [4, 15], we use the defect correction iteration as a finite process rather than compute its limit. To further improve the efficiency, we use few (say, 2 or 3,) $\mathcal{W}$-cycles to approximate $\left(\mathcal{L}^h\right)^{-1}$ in the defect correction procedures. The overall defect correction procedure we propose is summarized in Algorithm 3.

https://doi.org/10.4208/nmtma.2015.w09si Published online by Cambridge University Press

Algorithm 3. Defect Correction Procedure.

1. $\boldsymbol{x}_0^h = \texttt{W_ow}(\mathcal{L}^h, \boldsymbol{b}^h, \mathbf{0})$,
2. **for** $k = 1, \cdots, \texttt{MaxIt}$
3. Compute residual: $\boldsymbol{r}^h = \bar{\boldsymbol{b}}^h - \bar{\mathcal{L}}^h \boldsymbol{x}_{k-1}^h$,
4. Solve the residual equation approximately: $\boldsymbol{e}^h \leftarrow \texttt{W_ow}(\mathcal{L}^h, \boldsymbol{r}^h, \mathbf{0})$,
5. Update: $\boldsymbol{x}_k^h \leftarrow \boldsymbol{x}_{k-1}^h + \boldsymbol{e}^h$.
6. **end**

The defect correction procedure we present here is under rather simple settings that $\bar{\mathcal{L}}^h$ is discretized on the same rectangular grid used by the first order upwind MAC and also shares the same DoFs with the MAC scheme. In general, such defect correction procedure can be applied to more general high order discretizations on the same grid or other grids. In such case, transfer operators will be involved to transfer between the high order discretization and the first order upwind MAC scheme, and extra smoothing steps may be needed for the high order discretization where LSC-DGS smoother can be used. And it is better to use as a preconditioner in the auxiliary space preconditioning framework [29].

We emphasize that the primary goal of applying a simple defect correction procedure here is to improve the accuracy of numerical solution rather than the convergence order. For hyperbolic and convection-dominated problems, effective defect-correction procedure needs careful design though it is widely used in practice [20]. In [8, 17], careful studies show that the convergence behavior of defect correction procedure degenerates for both central difference scheme and a second order upwind scheme while still is satisfactory for upwind-biased schemes, for example, Fromm's scheme or van Leer's third-order scheme. Even for Fromm's scheme case, half-space analysis shows that the initial convergence rate may be slow when a first-order accurate operator $\mathcal{L}^h$ is used and the number of iterations required to reach the asymptotic convergence rate is grid-dependent. However, if the operator $\mathcal{L}^h$ and $\bar{\mathcal{L}}^h$ have the same order accuracy, the defect correction procedure demonstrates good efficiency. We refer to [9] for the details. Due to the complication of designing efficient defect correction procedure for convection-dominated problems, the choice of high accuracy discretization $\bar{\mathcal{L}}^h$, the convergence behavior of the defect correction procedure with the proposed $\mathcal{W}$-cycle multigrid with overweighting as $\left(\mathcal{L}^h\right)^{-1}$, and theoretical analysis (e.g. half-space analysis) of the overall defect correction scheme are subject to the future research.

https://doi.org/10.4208/nmtma.2015.w09si Published online by Cambridge University Press

5. Numerical experiment

In this section, we design numerical experiments to demonstrate the effectiveness of the LSC-DGS based multigrid methods (MG-LSC-DGS) for the Oseen equations using the first order upwind MAC scheme as well as the defect correction procedure. We mainly consider the following two examples.

Example 5.1. *Let Ω be the unit square $(0,1)\times(0,1)$. The analytical solution $\boldsymbol{u}$ and p are chosen as follows, so that $\int_\Omega p\,\mathrm{d}x\,\mathrm{d}y = 0$:*

$$\boldsymbol{u}(x,y) = \begin{pmatrix} (1-\cos(2\pi x))\sin(2\pi y) \\ \cos(2\pi y - 1)\sin(2\pi x) \end{pmatrix}, \quad p(x,y) = \frac{1}{3}x^3 - \frac{1}{12}.$$

and

$$\boldsymbol{a} = \begin{pmatrix} x\sin(2\pi y) \\ y\sin(2\pi x) \end{pmatrix}.$$

The viscosity $\mu = 10^{-12}$. The right hand side $\boldsymbol{f}$ is computed accordingly.

The second example is the standard leaky lid-driven cavity problem but with a prescribed flow [13].

Example 5.2. *Let Ω be the unit square $(0,1)\times(0,1)$. We choose*

$$\boldsymbol{a} = \begin{pmatrix} 8x(x-1)(1-2y) \\ 8(2x-1)y(y-1) \end{pmatrix}.$$

The viscosity $\mu = 10^{-6}$ and the external force $\boldsymbol{f} = 0$. Homogeneous Dirichlet boundary conditions are used for all velocity components except a positive unit horizontal velocity along the top edge is used.

For Example 5.1, the viscosity $\mu = 10^{-12}$ has no influence on the exact solution because the exact solution is chosen priorly and $\boldsymbol{f}$ is computed accordingly. Moreover, in the upwind scheme, numerical viscosity $\mu_h = h\|\boldsymbol{a}\|_\infty/2 \gg \mu$ is used on which the numerical solution depends. For Example 5.2, the exact solution depends on the viscosity $\mu = 10^{-6}$ although it is not known. The numerical solution of our first order upwind scheme depends on the numerical viscosity $\mu_h = h\|\boldsymbol{a}\|_\infty/2$ rather than μ.

We first test the performance of the MG method using the LSC-DGS smoother. We apply the $\mathcal{W}$-cycle MG method with overweighting. Here, in one step of LSC-DGS smoother for the Oseen problem, we use one step of symmetric Gauss-Seidel smoother for F^{-1} and $(BB')^{-1}$ respectively. For the overweighting scaling parameter, we choose $\alpha_u = 4/3$ and $\alpha_p = 1$ as mentioned before. The coarsest grid is $h = 1/4$. To show the contraction rate, we set the relative error tolerance to be $1e$-10. We also collect iteration steps for tolerance $1e$-4, which is enough for the first order scheme up to mesh size $h = 2^{-11}$.

https://doi.org/10.4208/nmtma.2015.w09si Published online by Cambridge University Press

Table 1: Number of iterations of MG-LSC-DGS for Example 5.1 ($\mathcal{W}$(1,1)-cycle).

h	$\mu_h = h\|\boldsymbol{a}\|_\infty/2$	tol = $1e$-10	Rate	tol = $1e$-4
1/64	1/128	20	0.305	7
1/128	1/256	19	0.283	6
1/256	1/512	18	0.262	6
1/512	1/1024	17	0.250	6
1/1024	1/2048	16	0.244	6
1/2048	1/4096	16	0.245	6

Table 2: Number of iterations of MG-LSC-DGS for Example 5.2 ($\mathcal{W}$(1,1)-cycle).

h	$\mu_h = h\|\boldsymbol{a}\|_\infty/2$	tol = $1e$-10	Rate	tol = $1e$-4
1/64	1/64	17	0.268	6
1/128	1/128	16	0.266	5
1/256	1/256	17	0.278	5
1/512	1/512	19	0.306	5
1/1024	1/1024	21	0.331	5
1/2048	1/2048	23	0.358	5

In Table 1 and 2, we show the number of iterations of the MG-LSC-DGS method for both examples. Here, the averaged "Rate" is computed as follows

$$\text{Rate} = \frac{1}{\#\text{steps}} \sum_{i=4}^{\#\text{steps}} \exp\left(\frac{\log(\|\mathbf{r_i}\|/\|\mathbf{r_4}\|)}{(i-3)}\right),$$

where $\|\mathbf{r_i}\|$ is the ℓ_2 norm of residual at the i-th step and #steps is the overall number of iterations. From these tables, we can see the number of iteration remains almost the same and it is robust with respect to the numerical viscosity μ_h. We want to comment that in [16], the same driven cavity example was considered and also is discretized by the MAC scheme. Smoothers based on HSS and AL splitting as well as B-S smoother were considered, and the overall $\mathcal{V}(1,1)$-cycle MG method is used as a preconditioner for FGMRes method. All the smoothers degenerate in performance with respect to decreasing viscosity (see Table III, IV, V, and VI in [16]). Here, we use $\mathcal{W}(1,1)$-cycle as a standard alone iterative solver for a first order upwind MAC scheme. The overall performance is robust with respect to both h and μ, which demonstrates the robustness of our MG-LSC-DGS method. One step of LSC-DGS smoother is simply one symmetric Gauss-Seidel (SGG) iteration for velocity and two SGS for pressure which is much cheaper than HSS, AL splitting and B-S smoothers. For the same tolerance 10^{-4}, our method only needs $5-6$ steps comparing $20-30$ steps for methods in [16]. In addition, we save several matrix-vector multiplications by not using a Krylov subspace method

https://doi.org/10.4208/nmtma.2015.w09si Published online by Cambridge University Press

as an outer iteration. This demonstrates the efficiency of our multigrid solver.

Because we use first order upwind MAC scheme, the accuracy of the solution might not be satisfactory though the MG method works well. Therefore, as discussed in Section 4, we use defect correction procedure to further improve the overall accuracy. In our numerical experiments, we choose the high order discretization $\bar{\mathcal{L}}^h$ to be the central difference MAC scheme for the true viscosity. Note that this discretization is second order consistent but unstable. We use it as a preliminary example to demonstrate the efficiency of the defect correction procedure.

Table 3: Defect correction procedure of Example 5.1 ($\mu = 10^{-12}$).

	Before defect correction		After defect correction	
h	$\|\boldsymbol{u}_I - \boldsymbol{u}_h\|$	$\|p_I - p_h\|$	$\|\boldsymbol{u}_I - \boldsymbol{u}_h\|$	$\|p_I - p_h\|$
1/64	2.59e-1	1.06e-1	3.93e-2	1.27e-2
1/128	1.52e-1	6.15e-2	1.67e-2	4.91e-3
1/256	8.36e-2	3.54e-2	8.28e-3	2.10e-3
1/512	4.69e-2	2.06e-2	4.22e-3	9.71e-4
1/1024	2.63e-2	1.32e-2	2.19e-3	4.95e-4
1/2048	1.54e-2	9.35e-3	1.12e-3	2.63e-4

In Table 3, we consider the recirculating flow example (Example 5.1) and the defect correction procedure. Here, $(\mathcal{L}^h)^{-1}$ is replaced by 2 steps of $\mathcal{W}(1,1)$-cycle MG method using the LSC-DGS smoother and 6 steps of defect correction steps are applied (overall 12 steps of $\mathcal{W}(1,1)$-cycle). The quantity $\boldsymbol{u}_h, p_h$ are numerical approximation and $\boldsymbol{u}_I, p_I$ are interpolant of the true solutions at location of unknowns, respectively. The norm is the scaled l^2-norm of vectors $h\|\cdot\|_{l^2}$ which mimics the L^2-norm of corresponding functions. From the table, we can see that the defect correction procedure improves the accuracy (10 - 30 times better) even when we are using an unstable high order discretization and a very small viscosity $\mu = 10^{-12}$. This demonstrates the efficiency of the defect correction procedure. It should be mentioned that though the accuracy is improved, the overall convergence order is still first order. As discussed in the last paragraph of Section 4, for convection-dominated problems, we do not use an upwind-biased discretization in $\bar{\mathcal{L}}^h$ and $\mathcal{L}^h$ is only first oder accuracy, which may cause degenerated convergence behavior in the defect-correction procedure. We can expect the improvement of the convergence order if both $\bar{\mathcal{L}}^h$ and $\mathcal{L}^h$ are chosen properly and the proposed MG-LSC-DGS scheme is adjusted accordingly.

We do not show the defect correction results for the driven cavity example (Example 5.2) due to the following two reasons. First, we do not have an analytic solution to compare with. Second, for convection dominated problems have singularity, vortices, and/or boundary layers, such as the driven cavity problem, using unstable high order scheme or high order upwind scheme might not be appropriate (see, e.g. [8, 17]). Therefore, upwind-biased high order schemes and possibly adaptive grids should be

https://doi.org/10.4208/nmtma.2015.w09si Published online by Cambridge University Press

used for such cases. Moreover, stable high order schemes might be used as $\mathcal{L}^h$ in order to achieve full efficiency of the defect correction technique for convection-dominated problems as suggested in [9]. The investigation along this line subjects to future research.

Acknowledgments Chen was supported by NSF Grant DMS-1115961, DMS-1418732, and in part by Department of Energy prime award # DE-SC0006903. Wang was supported by 2010-2012 China Scholarship Council (CSC) and in part by Department of Energy prime award # DE-SC0006903. Hu and Xu are partially supported by NSF Grant DMS-1217142, Department of Energy Grant DE-SC0006903, and the Applied Mathematics Program within the Department of Energy Office of Advanced Scientific Computing Research as part of the Collaboratory on Mathematics for Mesoscopic Modeling of Materials (DE-SC0009249).

The valuable and careful comments offered by anonymous referees are gratefully acknowledged.

References

[1] M. Benzi, G. Golub, and J. Liesen. Numerical solution of saddle point problems. *Acta Numerica*, 14(1):1–137, 2005.
[2] D. Braess and R. Sarazin. An efficient smoother for the Stokes problem. *Applied Numerical Mathematics*, 23(1):3–19, 1997.
[3] A. Brandt, Multi-level adaptive solutions to boundary-value problems *Math. Comp.*, 31 (1977), pp. 333–390.
[4] A. Brandt. *Multigrid techniques: 1984 guide with applications to fluid dynamics*. Ges. für Mathematik u. Datenverarbeitung, 1984.
[5] A. Brandt and N. Dinar. *Multi-grid solutions to elliptic flow problems*. Inst. for Computer Applications in Science and Engineering, NASA Langley Research Center, 1979.
[6] A. Brandt and I. Yavneh. On multigrid solution of high-Reynolds incompressible entering flows. *Journal of computational physics*, 101(1):151–164, 1992.
[7] A. Brandt and I. Yavneh. Accelerated multigrid convergence and high-Reynolds recirculating flows. *SIAM Journal on Scientific Computing*, 14:607–607, 1993.
[8] J. Désidéri and P. Hemker. Convergence analysis of the defect-correction iteration for hyperbolic problems. *SIAM J. Sci. Comput.*, 16(1):88-118, 1995.
[9] B. Diskin and J. Thomas. Half-space analysis of the defect-correction method for Fromm discretization of convection. *SIAM J. Sci. Comput.*, 22(2):633-655, 2000.
[10] B. Diskin, J. Thomas, and R. Mineck. On quantitative analysis methods for multigrid solutions. *SIAM J. Sci. Comput.*, 27(1):108-129.
[11] H. Elman. Preconditioning for the steady-state Navier–Stokes equations with low viscosity. *SIAM Journal on Scientific Computing*, 20(4):1299–1316, 1999.
[12] H. Elman, V. Howle, J. Shadid, R. Shuttleworth, and R. Tuminaro. Block preconditioners based on approximate commutators. *SIAM Journal on Scientific Computing*, 27(5):1651–1668, 2006.
[13] H. Elman, D. Silvester, and A. Wathen. *Finite elements and fast iterative solvers: with applications in incompressible fluid dynamics*. Oxford University Press, USA, 2005.

https://doi.org/10.4208/nmtma.2015.w09si Published online by Cambridge University Press

[14] L. Fuchs and H. Zhao. Solution of three-dimensional viscous incompressible flows by a multi-grid method. *International journal for numerical methods in fluids*, 4(6):539–555, 1984.
[15] W. Hackbusch. Multi-grid methods and applications, vol. 4 of springer series in computational mathematics, 1985.
[16] S. Hamilton, M. Benzi, and E. Haber. New multigrid smoothers for the Oseen problem. *Numerical Linear Algebra with Applications*, (February):557–576, 2010.
[17] P. Hemker and J. Désidéri. Convergence behavior of defect correction for hyperbolic equations. *Journal of Computational and Applied Mathematics*, 45:357-365, 1993.
[18] V. John. Higher order finite element methods and multigrid solvers in a benchmark problem for the 3D Navier–Stokes equations. *International Journal for Numerical Methods in Fluids*, 40(6):775–798, 2002.
[19] V. John and G. Matthies. Higher-order finite element discretizations in a benchmark problem for incompressible flows. *International Journal for Numerical Methods in Fluids*, 37(8):885–903, 2001.
[20] D. Mavriplis. Unstructured grid techniques. *Annu. Rev. Fluid. Mech.*, 29:473-514, 1997.
[21] C. Oosterlee, F. Gaspar. T. Washio, and R. Wienands. Multigrid line smoothers for high order upwind discretizations of convection-dominated problems. *Journal of Computational Physics*, 1:274–307, 1998.
[22] C. Oosterlee and F. Lorenz. Multigrid methods for the Stokes system. *Computing in science & engineering*, 8(6):34–43, 2006.
[23] C. Oosterlee and T. Washio. Krylov subspace acceleration of nonlinear multigrid with application to recirculating flows. *SIAM J. Sci. Comput.*, 21(5):1670–1690, 2000.
[24] J. Thomas. B. Diskin, and A. Brandt. Textbook multigrid efficiency for the incompressible navier-stokes equations: High reynolds number wakes and boundary layers. Computers & Fluids, 30(7-8):853-874, 2001.
[25] S. Vanka. Block-implicit multigrid solution of Navier-Stokes equations in primitive variables. *Journal of Computational Physics*, 65(1):138–158, 1986.
[26] M. Wang and L. Chen. Multigrid Methods for the Stokes Equations using Distributive Gauss-Seidel Relaxations based on the Least Squares Commutator. *Journal of Scientific Computing*, Feb. 2013.
[27] G. Wittum. Multi-grid methods for Stokes and Navier-Stokes equations. *Numerische Mathematik*, 54(5):543–563, 1989.
[28] G. Wittum. On the convergence of multi-grid methods with transforming smoothers. *Numerische Mathematik*, 57(1):15–38, 1990.
[29] J. Xu. The auxiliary space method and optimal multigrid preconditioning techniques for unstructured grids. *Computing*, 56(3):215–235, 1996.
[30] I. Yavneh. Coarse-grid correction for nonelliptic and singular perturbation problems. *SIAM J. Sci. Comput.*, 19(5):1682-1699, 1998.
[31] I. Yavneh, C. Venner, and A. Brandt Fast multigrid solution of the advection problem with closed characteristics. *SIAM J. Sci. Comput.*, 19(1):111-125, 1998.
[32] P. De Zeeuw. Matrix-dependent prolongations and restrictions in a blackbox multigrid solver, *J. Comput. Appl. Math.*, 33:1-27, 1990.
[33] L. Zhang. A second-order upwinding finite difference scheme for the steady navier-stokes equations in primitive variables in a driven cavity with a multigrid solver. *M2AN*, 24:133–150, 1990.

https://doi.org/10.4208/nmtma.2015.w09si Published online by Cambridge University Press